Published in final edited form as:

J Neurochem. 2019 March ; 148(5): 612–624. doi:10.1111/jnc.14545.

Astrocytes in Juvenile Neuronal Ceroid Lipofuscinosis (CLN3) display metabolic and calcium signaling abnormalities

Megan E. Bosch[1], **Tammy Kielian**[2,*]

[1]Departments of Pharmacology and Experimental Neuroscience, University of Nebraska Medical Center, Omaha, NE 68198

[2]Departments of Pathology and Microbiology, University of Nebraska Medical Center, Omaha, NE 68198

Abstract

Juvenile Neuronal Ceroid Lipofuscinosis (JNCL) is a lysosomal storage disease caused by autosomal recessive mutations in *CLN3*. Children with JNCL experience progressive visual, cognitive, and motor deterioration with a decreased life expectancy (late teens-early 20s). Neuronal loss is thought to occur, in part, via glutamate excitotoxicity; however, little is known about astrocyte glutamate regulation in JNCL. Spontaneous Ca^{2+} oscillations were reduced in murine $Cln3^{\Delta ex7/8}$ astrocytes, which were also observed following glutamate or cytokine exposure. Astrocyte glutamate transport is an energy-demanding process and disruptions in metabolic pathways could influence glutamate homeostasis in $Cln3^{\Delta ex7/8}$ astrocytes. Indeed, basal mitochondrial respiration and ATP production were significantly reduced in $Cln3^{\Delta ex7/8}$ astrocytes. These changes were not attributable to reduced mitochondria, since mitochondrial DNA levels were similar between WT and $Cln3^{\Delta ex7/8}$ astrocytes. Interestingly, despite these functional deficits in $Cln3^{\Delta ex7/8}$ astrocytes, glutamate transporter expression and glutamate uptake were not dramatically affected. Concurrent with impaired astrocyte metabolism and Ca^{2+} signaling, murine $Cln3^{\Delta ex7/8}$ neurons were hyper-responsive to glutamate, as reflected by heightened and prolonged Ca^{2+} signals. These findings identify intrinsic metabolic and Ca^{2+} signaling defects in $Cln3^{\Delta ex7/8}$ astrocytes that may contribute to neuronal dysfunction in CLN3 disease.

Keywords

Astrocyte; CLN3; mitochondrial dysfunction; calcium signaling

[*]**Corresponding Author:** Tammy Kielian, Ph.D., University of Nebraska Medical Center, Department of Pathology and Microbiology, 985900 Nebraska Medical Center, Omaha, NE 68198-5900, Phone: (402) 559-8002, FAX: (402) 559-5900, tkielian@unmc.edu.

AUTHOR CONTRIBUTIONS

Conceptualization, MEB and TK; Investigation, MEB; Writing – Original Draft, MEB; Writing – Review & Editing, MEB and TK; Funding Acquisition, TK and MEB; Supervision, TK.

CONFLICT OF INTEREST

Tammy Kielian is a Deputy Chief Editor for the *Journal of Neurochemistry*.

Introduction

Juvenile Neuronal Ceroid Lipofuscinosis (JNCL), or CLN3 disease, is a pediatric lysosomal storage disorder afflicting an estimated 1 in every 100,000 live births (The International Batten Disease Consortium 1995, Jalanko & Braulke 2009, Schultz et al. 2011). Children appear healthy until the onset of disease symptoms between the ages of 5-10 that initiates as vision loss, followed by seizures, dementia, and motor and cognitive decline, with premature death by the late teens to-early 20s (The International Batten Disease Consortium 1995, Aberg et al. 2000, Rakheja et al. 2007). JNCL is caused by autosomal recessive mutations in *CLN3* (The International Batten Disease Consortium 1995, Williams & Mole 2012). Most common is a 1.02kb deletion that occurs in approximately 85% of mutated *CLN3* alleles, which is considered to encode a truncated protein that is minimally expressed and/or rapidly degraded (The International Batten Disease Consortium 1995, Getty & Pearce 2011). While its function still remains unknown, CLN3 has been implicated in multiple cellular processes, including lysosomal acidification, amino acid transport, mitochondrial function, and intracellular Ca^{2+} regulation (Chandrachud et al. 2015, Chang et al. 2007, Fossale et al. 2004, Kyttala et al. 2006, Ramirez-Montealegre & Pearce 2005).

CLN3 pathology is characterized by the accumulation of lysosomal inclusions in all cell types, with neurons most dramatically affected (Haltia 2003, Williams et al. 2006). Current evidence suggests that inclusions are not a direct cause of neuron death, since many inclusion-positive neurons are not lost during the disease (Cooper et al. 2015, Cotman et al. 2002). In terms of alternative possibilities, previous studies have suggested that disruptions in glial function and loss of neuron homeostatic support may contribute to neuron dysfunction in JNCL. In particular, astrocytes have increased hemichannel (HC) opening during early disease that can serve as a conduit for ATP, Ca^{2+}, and glutamate release (Burkovetskaya 2014, Orellana et al. 2011). *Cln3*-deficient astrocytes have also been reported to produce less neurotropic factors, which coincided with a negative impact on neuronal survival (Parviainen et al. 2017). In addition, $Cln3^{\Delta ex7/8}$ microglia exist in a primed pro-inflammatory state, producing exaggerated levels of several cytokines, such as IL-1β and TNF-α, that can potentiate astrocyte HC opening and augment glutamate release, disrupting cellular homeostasis (Bosch & Kielian 2014, Xiong & Kielian 2013). These data are supported by the finding that glutamate levels are elevated in the brains of both JNCL patients as well as *Cln3* mouse models (Kovacs & Pearce 2008, Pears et al. 2005, Sitter et al. 2004, Anzai et al. 2006). The underlying mechanisms responsible for elevated glutamate in the JNCL brain remain to be identified, but collectively the available evidence suggests a disruption in vital astrocyte homeostatic functions is a contributing factor.

Astrocytes are the primary cell type responsible for regulating extracellular glutamate levels to maintain neuronal homeostasis (Sofroniew & Vinters 2010). Astrocyte projections surround the tripartite synapse and remove glutamate primarily through the Na^{2+}-dependent glutamate symporters glutamate-aspartate transporter (GLAST) and glutamate transporter 1 (GLT-1) (Beart & O'Shea 2007). Glutamate transporter action is an energy-demanding process, which requires the Na^{+}/K^{+} ATPase to produce large quantities of ATP (Stobart & Anderson 2013). Disruption in any step of the glutamate uptake pathway can result in increased synaptic glutamate concentrations that are capable of inducing neuron

excitotoxicity (Eid et al. 2004, Vercellino et al. 2007). In addition to CLN3 disease, alterations in glutamate homeostasis have been reported in several neurodegenerative disorders, including Alzheimer's disease, Parkinson's disease, and other lysosomal storage disorders, such as Niemann-Pick type C (Assous et al. 2014, Byun et al. 2006, Kulijewicz-Nawrot et al. 2013, van der Hel et al. 2005). Besides maintaining CNS metabolic homeostasis, astrocytes control neurotransmitter release and neuronal signaling, in part, by regulating Ca^{2+} levels at the synapse (Eroglu & Barres 2010, Li et al. 2013, Ullian et al. 2001). Astrocytes interpret neuronal signaling patterns and communicate to surrounding cells via Ca^{2+} waves, which act as a glial signaling system for the propagation of both paracrine and distant signals in the CNS (Bazargani & Attwell 2016, Scemes & Giaume 2006). Strong evidence has emerged suggesting that perturbations in astrocyte signaling Ca^{2+} contribute to neuronal hyperactivity, loss of astrocyte homeostatic support, and disruption of the extracellular milieu (Manning & Sontheimer 1997, Seifert et al. 2006).

Here we present evidence of intrinsic abnormalities in *Cln3*$^{\Delta ex7/8}$ astrocytes that may account, in part, for neuroexcitotoxicity in the CLN3 brain. Specifically, *Cln3*$^{\Delta ex7/8}$ astrocytes displayed reduced Ca^{2+} oscillations, impaired mitochondrial activity, and ATP production. However, despite these intrinsic defects, glutamate transporter expression and glutamate uptake were not significantly different between *Cln3*$^{\Delta ex7/8}$ and WT astrocytes. *Cln3*$^{\Delta ex7/8}$ neurons were hyper-responsive to glutamate, exhibiting elevated and prolonged Ca^{2+} signals. Collectively, these findings reveal mechanisms that could impair astrocyte-neuron glutamate crosstalk and contribute to neuronal excitotoxicity during CLN3 disease progression.

Materials and Methods

Animals.

Male and female *Cln3*$^{\Delta ex7/8}$ mice (C57BL/6 background, The Jackson Laboratory; RRID:IMSR_JAX:004685), which harbor the same 1.02 kb deletion spanning exons 7 and 8 that occurs in approximately 85% of mutated *CLN3* alleles in humans, were used for preparing primary astrocyte and neuron cultures (Cotman et al 2002). Both sexes of C57BL/6 mice were used as wild type (WT) controls (The Jackson Laboratory; RRID:IMSR_JAX:000664). Adult mice were bred under standard cage density conditions with 2 females and 1 male per cage with ad libitum access to food and water. For generating timed pregnant mice for primary neuronal cultures, the male was removed from females after a 24 h period, which was considered gestational day 1. Pregnancy was verified by the presence of vaginal plugs and/or weight gain. This study was conducted in strict accordance with the recommendations in the *Guide for the Care and Use of Laboratory Animals* of the National Institutes of Health and complies with the ARRIVE guidelines. The animal use protocol was approved by the Institutional Animal Care and Use Committee of the University of Nebraska Medical Center (11-074-08-EP) and was not pre-registered. There was no randomization of animals for these studies; mouse embryos or pups were sacrificed from an individual timed pregnant female or litter, respectively, for preparing primary neuron and astrocyte cultures.

Experimental overview.

No blinding was performed during the preparation of primary cell cultures or during the course of experiments. There were no differences in sample sizes for each experiment between the beginning and end of the study.

Astrocyte and neuron cultures.

Primary WT and *Cln3*$^{\Delta ex7/8}$ astrocytes were prepared from mouse pups at postnatal days 2-3 as previously described (Esen et al 2007). Mouse pups were euthanized with an overdose of inhaled isoflurane and death was confirmed by the absence of heartbeat. For euthanasia, isoflurane was added to the bottom of a glass desiccator jar and pups separated from the irritating anesthetic by a 1 cm-thick porcelain base. Following isoflurane euthanasia, the cortex was dissected from both male and female pups and immediately placed in ice-cold phosphate buffered saline (PBS) supplemented with 2% fetal bovine serum (FBS; Atlanta Biologicals; Cat. #S11550). Cells were disassociated with trypsin and following several washes plated in 75mm^2 flasks (one brain per flask) in Dulbecco Modified Eagle Medium (DMEM, 4.5 g/L glucose; Hyclone/ThermoFisher; Cat. #SH3002202) supplemented with 10% FBS, 200μM L-glutamine (Corning; Cat. #25-005-Cl), oxaloacetic acid/sodium pyruvate/insulin (OPI; Sigma; Cat. #O5003), 1X penicillin/streptomycin/fungizone (Corning; Cat. #30-004-Cl), and 100μM L-leucine methyl ester (L-LME; Sigma; Cat. #L1002) to induce microglial apoptosis and prevent their expansion. Upon reaching confluence (approximately 7-10 days *in vitro*; DIV), astrocytes were passaged every 3-4 days and were not used for experiments past three passages (DIV 30-40). To ensure the removal of residual, loosely adherent microglia, flasks were shaken at 200 rpm for 12 h prior to plating. This approach resulted in astrocyte purity of > 95% as revealed by glial fibrillary acidic protein (GFAP) staining.

Primary cultures of WT and *Cln3*$^{\Delta ex7/8}$ cortical neurons were prepared as previously described (Xiong & Kielian 2013). Timed pregnant mice were sacrificed using an overdose of inhaled isoflurane, as described above, and embryos (embryonic day 16; E16) were collected post-mortem. The cortex was dissected from E16 embryos and following trypsin treatment, cells were plated on polyethylenimine (PEI; Sigma; Cat. #P3143)-coated 10mm^2 dishes at 10^6 cells/dish. Medium was changed 4 h after plating to remove non-adherent cells. Neurons were grown in Neurobasal medium (Life Technologies; Cat. #21103-0449) supplemented with L-glutamine, penicillin/streptomycin/fungizone, and B-27 supplement (ThermoFisher; Cat. #17504044). Cultures were treated with 1 μM cytosine arabinoside (AraC; Sigma; Cat. #C6645-100) to prevent glial expansion, beginning on DIV 3 and continuing until use in experiments. Every 3 days, half of the spent culture medium was replaced with fresh medium and cultures were not utilized until after DIV 10. Cultures contained a heterogeneous population of neurons in an effort to recapitulate neuronal heterogeneity within the cortex. The composition of excitatory and interneuron populations was not determined.

Seahorse mitochondrial stress and glycolysis assays.

Primary WT and *Cln3*$^{\Delta ex7/8}$ astrocytes were plated at 2x10^4 cells per well in 96-well plates and incubated for 12 h prior to treatment with combinations of tumor necrosis factor-α

(TNF-α) and interleukin-1β (IL-1β) (PeproTech; Cat. # 314-10B and 211-11B, respectively; 10ng/ml each) or C6 ceramide (5μM; Sigma; Cat. #H6524) and neuronal lysate (1:5 dilution) for 24 h. Neuronal lysate was prepared from primary C57BL/6 wild type E16 neurons after multiple freeze-thaw cycles as previously described, since our prior report revealed no significant differences in microglial responses to neuronal lysates from WT or *Cln3*$^{\Delta ex7/8}$ mice (Xiong & Kielian 2013). Prior to the start of metabolic assays, culture medium was replaced with sodium bicarbonate- and serum-free medium. Seahorse XF Cell Mito Stress Test Kit (Cat. #103015-100) and Seahorse XFp Glycolysis Stress Test Kit (Cat. #103017-100) protocols were performed according to the manufacturer's instructions (Agilent, Santa Clara, CA). For mitochondrial stress tests, oxygen consumption rate (OCR) was measured following sequential exposure to oligomycin (1μM; Sigma; Cat. #75351), carbonilcyanide *p*-triflouromethoxyphenylhydrazone (FCCP, 2μM; Sigma; Cat. #C2920), and rotenone (1μM; Sigma; Cat. #R8875). At the beginning of the assay, the Seahorse instrument measures changes in oxygen concentration in immediate proximity to cells to determine the baseline oxygen consumption rate. Next, oligomycin is injected to inhibit adenosine triphosphate (ATP) production by blocking ATP synthase. Following oligomycin treatment, FCCP is injected, which is a membrane uncoupler that causes an increase in oxygen consumption without ATP generation. Finally, the complex I inhibitor rotenone, is injected to completely block mitochondrial respiration. By sequentially inhibiting different stages of the electron transport chain, well-established algorithms can be used to calculate basal respiration, ATP production, maximal respiration, and non-mitochondrial oxygen consumption (Rogers et al. 2011, Tan et al. 2015).

To test mitochondrial function in neurons, primary WT and *Cln3*$^{\Delta ex7/8}$ neurons were plated at 5x10^4 cells per well in 96-well plates for 10 days prior to treatment for 24 h with combinations of TNF-α and IL-1β (10ng/ml each) or C6 ceramide (5μM) and neuronal lysate (1:5 dilution). For mitochondrial stress tests, oxygen consumption rate (OCR) was measured following sequential exposure to oligomycin (1μM), FCCP (1μM), and rotenone (1μM), whereupon mitochondrial respiration was calculated as described above for astrocytes.

To measure glycolytic activity, astrocytes were pre-incubated for 1 h in medium lacking sodium bicarbonate, serum, and glucose prior to initiating the assay to reduce intracellular glucose stores. Next, cells were sequentially exposed to glucose (2.5M; Sigma; Cat. #D6134), oligomycin (1μM), and 2-deoxy-D-glucose (100μM; Sigma; Cat. #D8375) and extracellular acidification rate (ECAR) measured. Total protein was quantified in each well following Seahorse assays to confirm lack of cell toxicity.

Mitochondrial DNA (mtDNA) content.

Total DNA was extracted from WT and *Cln3*$^{\Delta ex7/8}$ astrocytes or E16 neurons using a DNAeasy Blood and Tissue kit (Qiagen, Valencia, CA, Cat. #69504) according to the manufacturer's instructions. mtDNA content was quantified using TaqMan primer-probe sets for the mitochondrial-specific genes NADH dehydrogenase 3 (ND3; Mm04225292_g1) and cytochrome c oxidase subunit-1 (Cox-1; Mm04225243_g1) as well as nuclear DNA (glyceraldehyde 3-phosphate dehydrogenase; GAPDH; Mm99999915_g1) (all from

ThermoFisher) and analyzed using a BioRad CFX Connect Real Time system (BioRad). Results were expressed as the ratio of mtDNA (ND3 or Cox-1) to nuclear DNA (GAPDH).

Calcium signaling.

Primary WT and *Cln3*$^{\Delta ex7/8}$ neurons and astrocytes were prepared as described above and plated on 18mm PEI-coated glass coverslips. Cells were loaded for 30 min with the Ca^{2+} indicator dye 4-(6-Acetoxymethoxy-2,7-difluoro-3-oxo-9-xanthenyl)-4′-methyl-2,2′-(ethylenedioxy)dianiline-N,N,N′,N′-tetraacetic acid tetrakis(acetoxymethyl) ester (Fluo4-AM, 1μM; Life Technologies; Cat. #F14202) in the presence of artificial cerebral spinal fluid (ACSF; containing in mM: 124 NaCl, 26 $NaHCO_3$, 3 KCl, 2 $MgCl_2$, 2 $CaCl_2$, 1.25 NaH_2PO_4, 10 glucose, 0.5 ascorbic acid, 1.5 Na-pyruvate, 1 thiourea; pH 7.4, maintained by continuous bubbling with carbogen [95% O_2 and 5% CO_2]) and cells were continuously perfused with ACSF throughout the imaging period. For neurons, live cell imaging was performed for 1 min to acquire baseline fluorescence signals, whereupon cells were stimulated with 25nM glutamic acid (Sigma; Cat. #G8415) and images were captured every 5 sec for 10 min using AxioVision software (Zeiss; RRID:SCR_002677). For neurons, 3 dishes per experimental group were imaged (7-10 neurons per dish) and the experiment was replicated 3 times. For astrocytes, spontaneous Ca^{2+} oscillations with or without cytokine pre-treatment (TNF-α and IL-1β; 10ng/ml each for 24 h) were measured over a 5 min period with images taken every 5 sec for baseline measurements. Astrocytes were then stimulated with 10mM glutamate and intracellular Ca^{2+} signaling associated with the cell soma was quantified by changes in mean fluorescent intensity after normalization to baseline values. Three dishes per experimental group were imaged (20 astrocytes per dish) and the experiment was replicated 3-4 times.

Glutamate uptake assay.

Primary WT and *Cln3*$^{\Delta ex7/8}$ astrocytes were seeded at $2x10^4$ cells per well in 96-well plates and incubated for 12 h prior to treatment with combinations of TNF-α and IL-1β (10ng/ml each) or C6 ceramide (5μM) and neuronal lysate (1:5 dilution) for 24 h. To examine glutamate uptake efficiency, astrocytes were exposed to 1mM glutamic acid in phenol red-free DMEM (ThermoFisher; Cat. #31053-028), whereupon supernatants were collected at 30 min and 2 h following glutamate treatment. Glutamate concentrations were immediately analyzed using an Amplex Red Glutamic Acid assay kit according to the manufacturer's instructions (ThermoFisher, Cat. #A12221) with values normalized to the respective 1mM glutamate control at each time point.

Statistical analysis.

A Student's *t*-test was used to analyze paired data sets of *Cln3*$^{\Delta ex7/8}$ and WT astrocytes for Ca^{2+} oscillations, Seahorse metabolic assays, mtDNA content, and neuronal Ca^{2+} oscillations using GraphPad Prism version 6.04 (San Diego, CA; RRID:SCR_002798). An assessment of data normality and a test to identify outliers were not performed for the datasets. For all analysis $p < 0.05$ was considered statistically significant.

Results

CLN3 mutation perturbs astrocyte Ca^{2+} oscillations.

Astrocytes utilize Ca^{2+} signaling to communicate with surrounding cells as well as regulate synaptic firing. Glutamate released from neurons activates astrocyte glutamate transporters and triggers an increase in astrocytic intracellular Ca^{2+} (Dani et al. 1992, Volterra et al. 2014). Elevated intracellular Ca^{2+} in astrocytes can activate multiple glutamate regulatory pathways, including trafficking of GLAST transporters to the membrane, mobilizing mitochondria to increase energy production, and increased Na^{+}-Ca^{2+} exchange pump activity to reduce K^{+} levels and neuronal firing (Bazargani & Attwell 2016, Mashimo et al. 2010, Stephen et al. 2014, Wang et al. 2012). Unchecked neuronal activity from impaired astrocyte regulation can increase glutamate concentrations, further potentiating glutamate dysregulation. To determine whether Ca^{2+} transients are perturbed in *Cln3*$^{\Delta ex7/8}$ astrocytes, live-cell Ca^{2+} imaging was performed. *Cln3*$^{\Delta ex7/8}$ astrocytes displayed decreased spontaneous Ca^{2+} oscillations under resting conditions, which was also observed when cells were exposed to proinflammatory cytokines that have previously been shown to be over-produced by *Cln3*$^{\Delta ex7/8}$ microglia (Figure 1) (Xiong & Kielian 2013). Following the assessment of basal spontaneous Ca^{2+} activity, astrocytes were exposed to glutamate to model extracellular neuronal signaling. Glutamate treatment increased intracellular Ca^{2+} in both WT and *Cln3*$^{\Delta ex7/8}$ astrocytes compared to baseline; however, levels were still significantly reduced in *Cln3*$^{\Delta ex7/8}$ cells (Figure 1). A single astrocyte is capable of simultaneously regulating multiple synapses, while at the same time one neuron may have its synapses enveloped by multiple astrocytes. Therefore, the reduction in *Cln3*$^{\Delta ex7/8}$ astrocyte Ca^{2+} signaling may not only have intrinsic effects or regulate local neuronal activity, but could also disrupt larger signaling networks.

Mitochondrial respiration is impaired in *Cln3*$^{\Delta ex7/8}$ astrocytes.

During periods of robust neuronal activity, astrocyte energy demands increase to maintain homeostatic functions (Stobart & Anderson 2013). Although neurons possess the highest metabolic requirements in the CNS, astrocytes account for approximately 20% of the energy usage in the brain during consciousness (Allaman et al. 2015). Astrocytes must maintain mitochondrial and glycolytic function to regulate neurotransmitter levels, ion homeostasis, and synaptic activity. Previous studies support mitochondrial dysfunction in JNCL, including increased mitochondrial oxidative stress molecules, mitochondrial membrane depolarization, and alterations in mitochondrial morphology (Cao et al. 2011, Chandrachud et al. 2015, Fossale et al. 2004, Hong et al. 2016, Kang et al. 2013). However, most of these studies were conducted with an immortalized *Cln3*$^{\Delta ex7/8}$ cerebellar cell line and none have examined mitochondrial activity in real-time in astrocytes. Here we utilized Seahorse bioassays to determine whether *Cln3*$^{\Delta ex7/8}$ astrocytes display defects in mitochondrial respiration. Under resting conditions, both basal respiration and ATP production were significantly reduced in *Cln3*$^{\Delta ex7/8}$ astrocytes (Figure 2A and B, respectively). Mitochondrial defects in *Cln3*$^{\Delta ex7/8}$ astrocytes were also evident when cells were exposed to JNCL danger signals (ceramide + neuronal lysate) or proinflammatory cytokines (TNF-α + IL-1β; Figure 2A and B). These mitochondrial defects could be attributed, in part, to dampened intracellular Ca^{2+} in *Cln3*$^{\Delta ex7/8}$ astrocytes, since mitochondrial respiration and

ATP production are Ca^{2+}-dependent and the failure to raise intracellular Ca^{2+} in *Cln3*$^{\Delta ex7/8}$ cells would be expected to interfere with mitochondrial function. Importantly, total protein concentrations were equivalent between WT and *Cln3*$^{\Delta ex7/8}$ astrocytes pre/post assay, indicating lack of toxicity (data not shown).

To determine whether defective mitochondrial activity in *Cln3*$^{\Delta ex7/8}$ astrocytes was due to alterations in mitochondrial abundance, mtDNA was quantified. Examination of two mitochondrial-specific genes, ND3 and Cox-1, revealed no significant differences in mtDNA content between WT and *Cln3*$^{\Delta ex7/8}$ astrocytes (Figure 2C). These results further support the significance of the observed oxidative phosphorylation (Ox Phos) defects in *Cln3*$^{\Delta ex7/8}$ astrocytes, which are independent of mitochondrial abundance. Without sufficient ATP generation in the face of high neuronal activity, *Cln3*$^{\Delta ex7/8}$ astrocytes may be unable to regulate the CNS extracellular milieu.

In instances of increased neuronal activity or distress, astrocytes augment glycolysis to produce more ATP. Since mitochondrial metabolism and ATP production were reduced in *Cln3*$^{\Delta ex7/8}$ astrocytes, we next examined whether cells shift to a more glycolytic profile to compensate. No significant differences in glycolytic rates were observed between *Cln3*$^{\Delta ex7/8}$ and WT astrocytes (Figure 3). This indicates that *Cln3*$^{\Delta ex7/8}$ astrocytes do not compensate for the reduction in mitochondrial ATP production by augmenting glycolytic pathways.

Properly functioning mitochondria and metabolic pathways are critical for neuronal functions, such as neurotransmission and Ca^{2+} signaling. To determine if *CLN3* mutation alters mitochondrial activity in neurons, Seahorse assays were performed using primary cortical neurons from WT and *Cln3*$^{\Delta ex7/8}$ mice. No significant changes in basal respiration or ATP production were detected under resting conditions between *Cln3*$^{\Delta ex7/8}$ and WT neurons (Supplemental Figure 1A and B). Similar results were observed when neurons were pre-treated for 24 h with cytokines (TNF-α + IL-1β) or danger signals (ceramide + neuronal lysate) (Supplemental Figure 1A and B). While a trend towards reduced mitochondrial activity was observed in *Cln3*$^{\Delta ex7/8}$ neurons, this was inconsistent and should be viewed with caution, since mtDNA levels were reduced in *Cln3*$^{\Delta ex7/8}$ neurons compared to WT (Supplemental Figure 1C).

Glutamate transporter expression and uptake are not significantly altered in *Cln3*$^{\Delta ex7/8}$ astrocytes.

The excitatory neurotransmitter glutamate is tightly regulated in the CNS and the pathways responsible for maintaining glutamate homeostasis are highly conserved (Kanai & Hediger 2003, Kim et al. 2011). Disruptions in glutamate regulation have been implicated in CLN3 disease, where glutamate levels are elevated in *Cln3* mouse models and treatment with NMDA or AMPA receptor antagonists improved motor function (Assous et al. 2014, Byun et al. 2006, Kovacs & Pearce 2008, Kovacs et al. 2012, Pears et al. 2005, Sitter et al. 2004). To explore the possibility of intrinsic alterations in glutamate transport in *Cln3*$^{\Delta ex7/8}$ astrocytes, we first examined glutamate transporter expression by Western blot. No significant differences in either GLT-1 or GLAST expression were detected between WT and *Cln3*$^{\Delta ex7/8}$ astrocytes under resting conditions or following cytokine (TNF-α + IL-1β) or glutamate treatment (data not shown). To determine whether glutamate uptake was affected

in *Cln3*$^{\Delta ex7/8}$ astrocytes, cells were assessed for their ability to remove glutamate from the extracellular milieu using an Amplex Red glutamic acid assay. Following a 24 h pre-treatment period with danger signals (ceramide + neuronal lysate) or cytokines (TNF-α + IL-1β), astrocytes were exposed to glutamic acid (1mM), whereupon the amount of glutamate remaining in the supernatant at 30 min and 2 h was measured. Extracellular glutamate levels were similar between *Cln3*$^{\Delta ex7/8}$ and WT astrocytes in all treatment conditions (Figure 4). Collectively, the decreases in Ca^{2+} signaling and ATP production in *Cln3*$^{\Delta ex7/8}$ astrocytes do not significantly impact intrinsic glutamate regulatory pathways, instead suggesting possible defects in cell-cell communication with neurons.

Cln3$^{\Delta ex7/8}$ neurons are hyper-excitable to extracellular glutamate.

Neurons are the principle cell type lost in CLN3 disease, which is thought to result, in part, from glutamate excitotoxicity (Haltia 2003, Williams et al. 2006, Chattopadhyay et al. 2002, Pears et al. 2005, Pontikis et al. 2005). Hyper-excitable or uninhibited excitatory neurons are a primary cause of seizures, which is a hallmark of disease in CLN3 patients (Cavus et al. 2016). To investigate the sensitivity of *Cln3*$^{\Delta ex7/8}$ neurons to physiological glutamate concentrations at the synaptic cleft (i.e. ~25nM) (Dzubay & Jahr 1999, Herman & Jahr 2007, Moussawi et al. 2011), live-cell Ca^{2+} imaging was performed. Glutamate application evoked a significant increase in intracellular Ca^{2+} in *Cln3*$^{\Delta ex7/8}$ neurons, reflecting their hyper-sensitivity to glutamate (Figure 5). After a 1 min stimulation period, glutamate washout was performed, which returned intracellular Ca^{2+} levels to baseline in WT but not *Cln3*$^{\Delta ex7/8}$ neurons, which is often used as an indication of impending excitotoxicity (Arundine & Tymianski 2004, Berdichevsky et al. 1983, Mattson 2007). Prior cytokine exposure (TNF-α and IL-1β) had no additive effect on the exaggerated Ca^{2+} flux in *Cln3*$^{\Delta ex7/8}$ neurons following glutamate stimulation (Supplemental Figure 2). Collectively, these studies suggest the existence of autonomous and non-cell autonomous mechanisms that may lead to glutamate dysregulation in CLN3 disease via impaired neuron and astrocyte activity. By extension, since *Cln3*$^{\Delta ex7/8}$ neurons are hyper-responsive to glutamate this could perpetuate glutamate release, which would ultimately lead to excitotoxicity and neuron death that is reminiscent of CLN3 disease.

Discussion

Although *CLN3* mutations were identified as the cause of JNCL in 1995, the precise function of CLN3 remains unknown (The International Batten Disease Consortium 1995, Kyttala et al. 2006). To date, CLN3 has been implicated in multiple processes critical for maintaining cellular homeostasis as well as dampening microglial proinflammatory activity (Chandrachud et al. 2015, Chang et al. 2007, Fossale et al. 2004, Kyttala et al. 2006, Ramirez-Montealegre & Pearce 2005, Xiong & Kielian 2013). Earlier studies have focused on the accumulation of lysosomal storage material within neurons, a hallmark of disease pathology and progression (The International Batten Disease Consortium 1995, Haltia 2003, Williams et al. 2006). However, there is little evidence directly implicating lysosomal inclusions as the cause of neuronal death (Bronson et al. 1993, Finn et al. 2011). For this reason, we chose to investigate other pathways that could contribute to neurodegeneration that is a hallmark of CLN3 disease.

One such pathway is glutamate regulation, which has been implicated as one mode of neurotoxicity in JNCL (Kovacs & Pearce 2008, Pears et al. 2005, Sitter et al. 2004, Anzai et al. 2006). However, not much is known about the mechanisms contributing to aberrant glutamate regulation in JNCL or the role of astrocytes in this process. It is likely that astrocyte activity influences neuronal survival in JNCL based on previous studies reporting that activated astrocytes coincide with brain regions where neurons are eventually lost in *Cln3* mouse models (Pontikis et al. 2004, Pontikis et al. 2005) and recent evidence that $Cln3^{\Delta 1\text{-}6}$ astrocytes negatively impact neuron survival *in vitro* (Parviainen et al. 2017). Likewise, it has been shown that increased astrocyte hemichannel activity and reduced expression of the glutamate transporter GLAST and glutamine synthetase are apparent in the $Cln3^{\Delta ex7/8}$ brain, which supports the concept of disrupted astrocyte glutamate regulation and homeostatic functions in JNCL (Burkovetskaya 2014). Here we present a potential model to account for increased extracellular glutamate in the JNCL brain, primarily centered on astrocyte-neuron crosstalk, since intrinsic astrocyte glutamate pathways are not dramatically affected (Figure 6). Our findings differ from a recent study that reported impaired glutamate uptake in $Cln3^{\Delta 1\text{-}6}$ astrocytes (Parviainen et al. 2017). This discrepancy might be explained by the different *Cln3* mouse models used or that Parviainen et *al.* examined glutamate uptake under resting conditions, whereas our study examined astrocytes that were exposed to JNCL-relevant stimuli. Specifically, our laboratory utilized $Cln3^{\Delta ex7/8}$ knock-in mice that harbor the same mutation that is observed in approximately 85% of mutated *CLN3* alleles in JNCL patients (Cotman et al. 2002). In contrast, Parviainen et al. used $Cln3^{\Delta ex1\text{-}6}$ mice that lack the first six exons of *CLN3*, which may lead to some variations. Second, differences in astrocyte culture conditions can influence phenotypes. Along these lines, Parviainen et al. isolated astrocytes from mixed glial cultures in the presence of macrophage colony-stimulating factor (M-CSF) and granulocyte-macrophage colony-stimulating factor (GM-CSF), whereas our culture method enriched for astrocytes at the outset by limiting microglial expansion with L-leucine methyl ester, a widely used approach (Jebelli et al. 2015, Thiele et al. 1983), in the absence of growth factor supplementation. Therefore, the presence of growth factors during the culture period and initial contact with other glia may contribute to the differences in astrocyte glutamate phenotypes between the studies. In terms of the glutamate uptake assay, Parviainen et al. treated astrocytes with a higher concentration of glutamate (2mM) for a longer period of time (2 h), whereas in our study astrocytes were exposed to less glutamate (1mM) for a shorter period (1 h), and it is possible that our approach did not sufficiently stress the cells to detect differences. Nevertheless, it is important to note that both Parviainen et al. and our study reported Ca^{2+} defects in *Cln3* astrocytes. Although our prior report documented reduced glutamate transporter expression, this was assessed *in vivo* with the full complement of interacting cell types, and phenotypes were evident in $Cln3^{\Delta ex7/8}$ mice at 3-6 months of age (Burkovetskaya 2014). It is possible that glutamate dysregulation may be observed in $Cln3^{\Delta ex7/8}$ astrocytes isolated from the adult brain, although this was not examined in the current study. Although we attempted to model disease-like conditions by treating astrocytes with mediators reportedly elevated post-mortem in the brains of CLN3 patients (i.e. ceramide and cytokines), this does not completely replicate the disease milieu in the brain. Nevertheless, we did identify several novel metabolic phenotypes in $Cln3^{\Delta ex7/8}$ astrocytes that may precede changes in glutamate regulation. The extracellular signals responsible for potential defects in astrocyte-neuron

communication in *Cln3*$^{\Delta ex7/8}$ cells remain to be identified. Based on the existing literature, glutamate is a likely candidate, since glutamate levels are reportedly elevated in the CLN3 brain post-mortem as well as in *Cln3* mouse models (Brockmann et al. 1996, Kovacs & Pearce 2008, Pears et al. 2005, Salek et al. 2011). Our study has identified defects in both *Cln3*$^{\Delta ex7/8}$ astrocytes and neurons in response to glutamate, namely decreased Ca^{2+} signaling in astrocytes coupled with neuronal hyper-excitability. Besides glutamate sensitivity, a reduction in growth factors or molecules responsible for stabilizing neuronal synapses might be altered, such as thrombospondin-1 that has been implicated in other neurological disorders (Christopherson et al. 2005, Crawford et al. 2012, Liauw et al. 2008, Risher & Eroglu 2012). Additional studies are needed to identify the key molecules in astrocyte-neuron crosstalk that are perturbed in the context of *CLN3* mutation.

An interesting attribute of CLN3 disease that distinguishes it from other forms of Batten disease is the protracted nature of pathology (occurs over a period of 10-15 years) and the fact that disease symptoms do not typically manifest until around 5-10 years of age (Goebel & Wisniewski 2004, Mole et al. 1999). This suggests the existence of compensatory mechanisms to maintain CNS homeostasis until a disease threshold is achieved. Although the mechanisms responsible for this prolonged disease course are unknown, one possibility may be progressive glutamate accumulation that initially leads to excessive neuronal activity and ultimately cell death. This is also an attractive possibility from a clinical perspective, since seizures are often an early hallmark of CLN3 disease, which may be attributed to glutamate hyperactivity, followed by neuronal death that could be due to glutamate excitotoxicity (Augustine et al. 2015, Coulter & Eid 2012, Stobart & Anderson 2013). We found that *Cln3*$^{\Delta ex7/8}$ neurons were hyper-reactive in response to physiological glutamate concentrations at the synaptic cleft (Arundine & Tymianski 2004, Berdichevsky et al. 1983, Mattson 2007). By extension, not only do *Cln3*$^{\Delta ex7/8}$ neurons require less glutamate to be activated, but increased activation would augment glutamate release, perpetuating the pathological circuit (Figure 6). *Cln3*$^{\Delta ex7/8}$ neurons also maintained higher levels of intracellular Ca^{2+} following glutamate exposure, indicative of a longer activation state (Rueda et al. 2016). In addition, whereas intracellular Ca^{2+} levels in WT neurons returned to baseline within 1 min of stimulation, *Cln3*$^{\Delta ex7/8}$ neurons maintained exaggerated intracellular Ca^{2+} levels, which has been shown to precede excitotoxicity (Manning & Sontheimer 1997, Seifert et al. 2006). We recently reported that neuronal activity was exaggerated in the hippocampus and cortex of *Cln3*$^{\Delta ex7/8}$ mice between 1 and 4 months of age (Burkovetskaya et al. 2017), supporting the heightened neuronal responses presented here. A recent report also described neuronal perturbations in *Cln3*-deficient mice, but this was only examined at late stage disease (i.e. 14 months) (Grunewald et al. 2017). Based on heightened Ca^{2+} responses to glutamate, *Cln3*$^{\Delta ex7/8}$ neurons were expected to exhibit metabolic deficits. Interestingly, we found no significant differences in basal respiration or ATP production between WT and *Cln3*$^{\Delta ex7/8}$ neurons. This differs from a prior study with a *Cln3*$^{\Delta ex7/8}$ cerebellar granular cell line that reported significantly reduced ATP levels (Cao et al. 2011). Although a trend towards decreased mitochondrial function was observed, the results were inconsistent between experiments and the slight reductions may be explained by decreased mtDNA content in *Cln3*$^{\Delta ex7/8}$ neurons. Alternatively, it is possible that the heterogeneous population of cortical neurons examined here masked a subset-specific

phenotype that might manifest on a single cell basis. This is supported by previous studies demonstrating that *CLN3* mutation effects certain neuron populations (i.e. GABAergic interneurons) and brain regions (i.e. thalamus and somatosensory barrel field cortex) more than others (Pears et al. 2005, Pontikis et al. 2004, Pontikis et al. 2005).

Glutamate regulation is critical for maintaining optimal neuron-astrocyte signaling networks (Fonnum 1984, Li et al. 2013). This is an extremely energy-demanding process, requiring a constant supply of ATP that becomes even more pronounced during times of heightened neuronal activity (Stobart & Anderson 2013), as suggested by our findings of hyper-reactive $Cln3^{\Delta ex7/8}$ neurons. Using Seahorse metabolic assays, mitochondrial basal respiration and ATP production were significantly lower in $Cln3^{\Delta ex7/8}$ astrocytes, even at the resting state. Mitochondrial function was also impaired when $Cln3^{\Delta ex7/8}$ astrocytes were exposed to JNCL-relevant stimuli. Importantly, these changes were independent of mitochondrial numbers, since mtDNA content was similar between WT and $Cln3^{\Delta ex7/8}$ astrocytes. To the best of our knowledge, this is the first report to demonstrate disruptions in astrocyte mitochondrial function in the context of *CLN3* mutation.

Astrocytes utilize Ca^{2+} signaling to communicate with surrounding astrocytes and neurons, sense extracellular cues, and regulate synaptic activity (Eroglu & Barres 2010, Li et al. 2013, Parpura et al. 1994, Ullian et al. 2001). Here we show that $Cln3^{\Delta ex7/8}$ astrocytes have lower spontaneous Ca^{2+} oscillations under resting conditions and following exposure to danger signals/proinflammatory cytokines. Ca^{2+} transients were also significantly reduced in $Cln3^{\Delta ex7/8}$ astrocytes in response to extracellular glutamate. This finding agrees with a recent study showing decreased Ca^{2+} waves in $Cln3^{\Delta 1\text{-}6}$ astrocytes following ATP exposure (Parviainen et al. 2017), although responses to the JNCL-relevant stimuli tested here (i.e. glutamate and inflammatory cytokines) were not examined. Previous studies have shown that $Cln3^{\Delta ex7/8}$ astrocytes have significantly lower connexin expression coupled with decreased hemichannel activity *in vivo* as the disease progresses (Burkovetskaya et al. 2014). Since hemichannels from adjacent cells join to form gap junctions that are known to propagate Ca^{2+}, this may account for the significant decrease in Ca^{2+} oscillations in $Cln3^{\Delta ex7/8}$ astrocytes. By extension, if $Cln3^{\Delta ex7/8}$ astrocytes are less responsive to extracellular signals, unable to propagate Ca^{2+} signals to surrounding astrocytes, and are not able to properly regulate synaptic activity, $Cln3^{\Delta ex7/8}$ neurons would continue to fire and release more glutamate, resulting in the pathological propagation of a dysfunctional glutamate circuit in CLN3 disease.

In summary, our study supports the following model to account for neuronal hyper-excitability in the context of *CLN3* mutation (Figure 6). First, CLN3 loss leads to cell autonomous changes in neurons, resulting in hyper-sensitivity to low glutamate concentrations. Excessive excitatory activity in $Cln3^{\Delta ex7/8}$ neurons triggers heightened glutamate release into the synaptic cleft and the surrounding extracellular milieu. Persistent elevations in extracellular glutamate are known to further induce pre-existing neuroinflammatory pathways that trigger the release of cytotoxic mediators, inhibit cellular homeostatic functions, and induce apoptosis (Munhoz et al. 2008, Takaki et al. 2012, Vesce et al. 2007). Mitochondrial basal respiration, ATP production, and spontaneous Ca^{2+} oscillations were significantly reduced in $Cln3^{\Delta ex7/8}$ astrocytes, which can have a major

impact on cell signaling and synaptic activity. Without proper astrocytic regulation, synaptic firing can escalate in *Cln3*$^{\Delta ex7/8}$ neurons, which may augment glutamate release and perpetuate the pathological cycle. Ultimately, this could be one mechanism to account for eventual neuronal loss associated with CLN3 disease.

Supplementary Material

Refer to Web version on PubMed Central for supplementary material.

ACKNOWLEDGEMENTS

This work was supported by the UNMC Dean's Pediatric Research Fund and the UNMC Department of Pediatrics (to T.K.). M.E.B. was supported by a predoctoral fellowship from the National Institute of Neurological Disorders and Stroke (F31 NS093884-01A1). The authors thank Rachel Fallet for mouse colony management.

ABBREVIATIONS

ACSF	artificial cerebral spinal fluid
AraC	cytosine arabinoside
ARRIVE	Animal Research: Reporting of *In Vivo* Experiments
ATP	adenosine triphosphate
Ca^{2+}	calcium
CLN3	ceroid lipofuscinosis 3
Cox-1	cytochrome c oxidase subunit-1
DIV	day *in vitro*
DMEM	Dulbecco Modified Eagle Medium
E16	embryonic day 16
ECAR	extracellular acidification rate
FBS	fetal bovine serum
FCCP	carbonilcyanide *p*-triflouromethoxyphenylhydrazone
Fluo4-AM	4-(6-Acetoxymethoxy-2,7-difluoro-3-oxo-9-xanthenyl)-4′-methyl-2,2′-(ethylenedioxy)dianiline-N,N,N′,N′-tetraacetic acid tetrakis(acetoxymethyl) ester
GAPDH	glyceraldehyde 3-phosphate dehydrogenase
GFAP	glial fibrillary acidic protein
GLAST	glutamate-aspartate transporter
Gln	glutamine

Glu	glutamate
GLT-1	glutamate transporter 1
HC	hemichannel
IL-1β	interleukin-1β
JNCL	juvenile neuronal ceroid lipofuscinosis
L-LME	L-leucine methyl ester
mtDNA	mitochondrial DNA
ND3	NADH dehydrogenase 3
OCR	oxygen consumption rate
Ox Phos	oxidative phosphorylation
PEI	polyethylenimine
PBS	phosphate buffered saline
TNF-α	tumor necrosis factor-α
WT	wild type

References

(The International Batten Disease Consortium) Isolation of a novel gene underlying Batten disease, CLN3. (1995) Cell, 82, 949–957. [PubMed: 7553855]

Aberg L, Liewendahl K, Nikkinen P, Autti T, Rinne JO and Santavuori P (2000) Decreased striatal dopamine transporter density in JNCL patients with parkinsonian symptoms. Neurology, 54, 1069–1074. [PubMed: 10720276]

Allaman I, Belanger M and Magistretti PJ (2015) Methylglyoxal, the dark side of glycolysis. Front Neurosci, 9, 23. [PubMed: 25709564]

Anzai Y, Hayashi M, Fueki N, Kurata K and Ohya T (2006) Protracted juvenile neuronal ceroid lipofuscinosis--an autopsy report and immunohistochemical analysis. Brain Dev, 28, 462–465. [PubMed: 16503390]

Arundine M and Tymianski M (2004) Molecular mechanisms of glutamate-dependent neurodegeneration in ischemia and traumatic brain injury. Cellular and molecular life sciences : CMLS, 61, 657–668. [PubMed: 15052409]

Assous M, Had-Aissouni L, Gubellini P, Melon C, Nafia I, Salin P, Kerkerian-Le-Goff L and Kachidian P (2014) Progressive Parkinsonism by acute dysfunction of excitatory amino acid transporters in the rat substantia nigra. Neurobiology of disease, 65, 69–81. [PubMed: 24480091]

Augustine EF, Adams HR, Beck CA et al. (2015) Standardized assessment of seizures in patients with juvenile neuronal ceroid lipofuscinosis. Developmental medicine and child neurology, 57, 366–371. [PubMed: 25387857]

Bazargani N and Attwell D (2016) Astrocyte calcium signaling: the third wave. Nature neuroscience, 19, 182–189. [PubMed: 26814587]

Beart PM and O'Shea RD (2007) Transporters for L-glutamate: an update on their molecular pharmacology and pathological involvement. British journal of pharmacology, 150, 5–17. [PubMed: 17088867]

Berdichevsky E, Riveros N, Sanchez-Armass S and Orrego F (1983) Kainate, N-methylaspartate and other excitatory amino acids increase calcium influx into rat brain cortex cells in vitro. Neuroscience letters, 36, 75–80. [PubMed: 6134262]

Bosch M and Kielian T (2014) Hemichannels in neurodegenerative diseases: is there a link to pathology? Frontiers in cellular neuroscience, 8, 242. [PubMed: 25191227]

Brockmann K, Pouwels PJ, Christen HJ, Frahm J and Hanefeld F (1996) Localized proton magnetic resonance spectroscopy of cerebral metabolic disturbances in children with neuronal ceroid lipofuscinosis. Neuropediatrics, 27, 242–248. [PubMed: 8971744]

Bronson RT, Lake BD, Cook S, Taylor S and Davisson MT (1993) Motor neuron degeneration of mice is a model of neuronal ceroid lipofuscinosis (Batten's disease). Annals of neurology, 33, 381–385. [PubMed: 7683855]

Burkovetskaya M, Karpuk N and Kielian T (2017) Age-dependent alterations in neuronal activity in the hippocampus and visual cortex in a mouse model of Juvenile Neuronal Ceroid Lipofuscinosis (CLN3). Neurobiology of disease, 100, 19–29. [PubMed: 28042098]

Burkovetskaya M, Karpuk N, Xiong J, Bosch M, Boska M, Takeuchi H, Suzumur A, and Kielian T (2014) Evidence for aberrant astrocyte hemichannel activity in Juvenile Neuronal Ceroid Lipofuscinosis (JNCL). PLoS One.

Byun K, Kim J, Cho SY et al. (2006) Alteration of the glutamate and GABA transporters in the hippocampus of the Niemann-Pick disease, type C mouse using proteomic analysis. Proteomics, 6, 1230–1236. [PubMed: 16429462]

Cao Y, Staropoli JF, Biswas S, Espinola JA, MacDonald ME, Lee JM and Cotman SL (2011) Distinct early molecular responses to mutations causing vLINCL and JNCL presage ATP synthase subunit C accumulation in cerebellar cells. PLoS One, 6, e17118. [PubMed: 21359198]

Cavus I, Romanyshyn JC, Kennard JT et al. (2016) Elevated basal glutamate and unchanged glutamine and GABA in refractory epilepsy: Microdialysis study of 79 patients at the yale epilepsy surgery program. Annals of neurology, 80, 35–45. [PubMed: 27129611]

Chandrachud U, Walker MW, Simas AM et al. (2015) Unbiased Cell-based Screening in a Neuronal Cell Model of Batten Disease Highlights an Interaction between Ca2+ Homeostasis, Autophagy, and CLN3 Protein Function. The Journal of biological chemistry, 290, 14361–14380. [PubMed: 25878248]

Chang JW, Choi H, Kim HJ, Jo DG, Jeon YJ, Noh JY, Park WJ and Jung YK (2007) Neuronal vulnerability of CLN3 deletion to calcium-induced cytotoxicity is mediated by calsenilin. Human molecular genetics, 16, 317–326. [PubMed: 17189291]

Chattopadhyay S, Ito M, Cooper JD, Brooks AI, Curran TM, Powers JM and Pearce DA (2002) An autoantibody inhibitory to glutamic acid decarboxylase in the neurodegenerative disorder Batten disease. Human molecular genetics, 11, 1421–1431. [PubMed: 12023984]

Christopherson KS, Ullian EM, Stokes CC et al. (2005) Thrombospondins are astrocyte-secreted proteins that promote CNS synaptogenesis. Cell, 120, 421–433. [PubMed: 15707899]

Cooper JD, Tarczyluk MA and Nelvagal HR (2015) Towards a new understanding of NCL pathogenesis. Biochimica et biophysica acta, 1852, 2256–2261. [PubMed: 26026924]

Cotman SL, Vrbanac V, Lebel LA et al. (2002) Cln3(Deltaex7/8) knock-in mice with the common JNCL mutation exhibit progressive neurologic disease that begins before birth. Human molecular genetics, 11, 2709–2721. [PubMed: 12374761]

Coulter DA and Eid T (2012) Astrocytic regulation of glutamate homeostasis in epilepsy. Glia, 60, 1215–1226. [PubMed: 22592998]

Crawford DC, Jiang X, Taylor A and Mennerick S (2012) Astrocyte-derived thrombospondins mediate the development of hippocampal presynaptic plasticity in vitro. The Journal of neuroscience : the official journal of the Society for Neuroscience, 32, 13100–13110. [PubMed: 22993427]

Dani JW, Chernjavsky A and Smith SJ (1992) Neuronal activity triggers calcium waves in hippocampal astrocyte networks. Neuron, 8, 429–440. [PubMed: 1347996]

Dzubay JA and Jahr CE (1999) The concentration of synaptically released glutamate outside of the climbing fiber-Purkinje cell synaptic cleft. The Journal of neuroscience : the official journal of the Society for Neuroscience, 19, 5265–5274. [PubMed: 10377338]

Eid T, Thomas MJ, Spencer DD et al. (2004) Loss of glutamine synthetase in the human epileptogenic hippocampus: possible mechanism for raised extracellular glutamate in mesial temporal lobe epilepsy. Lancet, 363, 28–37. [PubMed: 14723991]

Eroglu C and Barres BA (2010) Regulation of synaptic connectivity by glia. Nature, 468, 223–231. [PubMed: 21068831]

Finn R, Kovacs AD and Pearce DA (2011) Altered sensitivity of cerebellar granule cells to glutamate receptor overactivation in the Cln3(Deltaex7/8)-knock-in mouse model of juvenile neuronal ceroid lipofuscinosis. Neurochemistry international, 58, 648–655. [PubMed: 21315126]

Fonnum F (1984) Glutamate: a neurotransmitter in mammalian brain. Journal of neurochemistry, 42, 1–11. [PubMed: 6139418]

Fossale E, Wolf P, Espinola JA et al. (2004) Membrane trafficking and mitochondrial abnormalities precede subunit c deposition in a cerebellar cell model of juvenile neuronal ceroid lipofuscinosis. BMC neuroscience, 5, 57. [PubMed: 15588329]

Getty AL and Pearce DA (2011) Interactions of the proteins of neuronal ceroid lipofuscinosis: clues to function. Cellular and molecular life sciences : CMLS, 68, 453–474. [PubMed: 20680390]

Goebel HH and Wisniewski KE (2004) Current state of clinical and morphological features in human NCL. Brain pathology, 14, 61–69. [PubMed: 14997938]

Grunewald B, Lange MD, Werner C et al. (2017) Defective synaptic transmission causes disease signs in a mouse model of juvenile neuronal ceroid lipofuscinosis. Elife, 6.

Haltia M (2003) The neuronal ceroid-lipofuscinoses. Journal of neuropathology and experimental neurology, 62, 1–13. [PubMed: 12528813]

Herman MA and Jahr CE (2007) Extracellular glutamate concentration in hippocampal slice. The Journal of neuroscience : the official journal of the Society for Neuroscience, 27, 9736–9741. [PubMed: 17804634]

Hong M, Song KD, Lee HK, Yi S, Lee YS, Heo TH, Jun HS and Kim SJ (2016) Fibrates inhibit the apoptosis of Batten disease lymphoblast cells via autophagy recovery and regulation of mitochondrial membrane potential. *In* Vitro Cell Dev Biol Anim, 52, 349–355.

Jalanko A and Braulke T (2009) Neuronal ceroid lipofuscinoses. Biochimica et biophysica acta, 1793, 697–709. [PubMed: 19084560]

Jebelli J, Piers T and Pocock J (2015) Selective Depletion of Microglia from Cerebellar Granule Cell Cultures Using L-leucine Methyl Ester. J Vis Exp, e52983.

Kanai Y and Hediger MA (2003) The glutamate and neutral amino acid transporter family: physiological and pharmacological implications. European journal of pharmacology, 479, 237–247. [PubMed: 14612154]

Kang S, Seo JH, Heo TH and Kim SJ (2013) Batten disease is linked to altered expression of mitochondria-related metabolic molecules. Neurochemistry international, 62, 931–935. [PubMed: 23524239]

Kim K, Lee SG, Kegelman TP et al. (2011) Role of excitatory amino acid transporter-2 (EAAT2) and glutamate in neurodegeneration: opportunities for developing novel therapeutics. Journal of cellular physiology, 226, 2484–2493. [PubMed: 21792905]

Kovacs AD and Pearce DA (2008) Attenuation of AMPA receptor activity improves motor skills in a mouse model of juvenile Batten disease. Experimental neurology, 209, 288–291. [PubMed: 17963751]

Kovacs AD, Saje A, Wong A, Ramji S, Cooper JD and Pearce DA (2012) Age-dependent therapeutic effect of memantine in a mouse model of juvenile Batten disease. Neuropharmacology, 63, 769–775. [PubMed: 22683643]

Kulijewicz-Nawrot M, Sykova E, Chvatal A, Verkhratsky A and Rodriguez JJ (2013) Astrocytes and glutamate homoeostasis in Alzheimer's disease: a decrease in glutamine synthetase, but not in glutamate transporter-1, in the prefrontal cortex. ASN neuro, 5, 273–282. [PubMed: 24059854]

Kyttala A, Lahtinen U, Braulke T and Hofmann SL (2006) Functional biology of the neuronal ceroid lipofuscinoses (NCL) proteins. Biochimica et biophysica acta, 1762, 920–933. [PubMed: 16839750]

Li D, Agulhon C, Schmidt E, Oheim M and Ropert N (2013) New tools for investigating astrocyte-to-neuron communication. Frontiers in cellular neuroscience, 7, 193. [PubMed: 24194698]

Liauw J, Hoang S, Choi M et al. (2008) Thrombospondins 1 and 2 are necessary for synaptic plasticity and functional recovery after stroke. J Cereb Blood Flow Metab, 28, 1722–1732. [PubMed: 18594557]

Manning TJ Jr. and Sontheimer H (1997) Spontaneous intracellular calcium oscillations in cortical astrocytes from a patient with intractable childhood epilepsy (Rasmussen's encephalitis). Glia, 21, 332–337. [PubMed: 9383042]

Mashimo M, Okubo Y, Yamazawa T, Yamasaki M, Watanabe M, Murayama T and Iino M (2010) Inositol 1,4,5-trisphosphate signaling maintains the activity of glutamate uptake in Bergmann glia. The European journal of neuroscience, 32, 1668–1677. [PubMed: 20958799]

Mattson MP (2007) Calcium and neurodegeneration. Aging Cell, 6, 337–350. [PubMed: 17328689]

Mole SE, Mitchison HM and Munroe PB (1999) Molecular basis of the neuronal ceroid lipofuscinoses: mutations in CLN1, CLN2, CLN3, and CLN5. Hum Mutat, 14, 199–215. [PubMed: 10477428]

Moussawi K, Riegel A, Nair S and Kalivas PW (2011) Extracellular glutamate: functional compartments operate in different concentration ranges. Front Syst Neurosci, 5, 94. [PubMed: 22275885]

Munhoz CD, Garcia-Bueno B, Madrigal JL, Lepsch LB, Scavone C and Leza JC (2008) Stress-induced neuroinflammation: mechanisms and new pharmacological targets. Braz J Med Biol Res, 41, 1037–1046. [PubMed: 19148364]

Orellana JA, Froger N, Ezan P, Jiang JX, Bennett MV, Naus CC, Giaume C and Saez JC (2011) ATP and glutamate released via astroglial connexin 43 hemichannels mediate neuronal death through activation of pannexin 1 hemichannels. Journal of neurochemistry, 118, 826–840. [PubMed: 21294731]

Parpura V, Basarsky TA, Liu F, Jeftinija K, Jeftinija S and Haydon PG (1994) Glutamate-mediated astrocyte-neuron signalling. Nature, 369, 744–747. [PubMed: 7911978]

Parviainen L, Dihanich S, Anderson GW et al. (2017) Glial cells are functionally impaired in juvenile neuronal ceroid lipofuscinosis and detrimental to neurons. Acta Neuropathol Commun, 5, 74. [PubMed: 29041969]

Pears MR, Cooper JD, Mitchison HM, Mortishire-Smith RJ, Pearce DA and Griffin JL (2005) High resolution 1H NMR-based metabolomics indicates a neurotransmitter cycling deficit in cerebral tissue from a mouse model of Batten disease. The Journal of biological chemistry, 280, 42508–42514. [PubMed: 16239221]

Pontikis CC, Cella CV, Parihar N et al. (2004) Late onset neurodegeneration in the Cln3−/− mouse model of juvenile neuronal ceroid lipofuscinosis is preceded by low level glial activation. Brain research, 1023, 231–242. [PubMed: 15374749]

Pontikis CC, Cotman SL, MacDonald ME and Cooper JD (2005) Thalamocortical neuron loss and localized astrocytosis in the Cln3Deltaex7/8 knock-in mouse model of Batten disease. Neurobiology of disease, 20, 823–836. [PubMed: 16006136]

Rakheja D, Narayan SB and Bennett MJ (2007) Juvenile neuronal ceroid-lipofuscinosis (Batten disease): a brief review and update. Current molecular medicine, 7, 603–608. [PubMed: 17896996]

Ramirez-Montealegre D and Pearce DA (2005) Defective lysosomal arginine transport in juvenile Batten disease. Human molecular genetics, 14, 3759–3773. [PubMed: 16251196]

Risher WC and Eroglu C (2012) Thrombospondins as key regulators of synaptogenesis in the central nervous system. Matrix Biol, 31, 170–177. [PubMed: 22285841]

Rogers GW, Brand MD, Petrosyan S, Ashok D, Elorza AA, Ferrick DA and Murphy AN (2011) High throughput microplate respiratory measurements using minimal quantities of isolated mitochondria. PLoS One, 6, e21746. [PubMed: 21799747]

Rueda CB, Llorente-Folch I, Traba J et al. (2016) Glutamate excitotoxicity and Ca2+-regulation of respiration: Role of the Ca2+ activated mitochondrial transporters (CaMCs). Biochimica et biophysica acta, 1857, 1158–1166. [PubMed: 27060251]

Salek RM, Pears MR, Cooper JD, Mitchison HM, Pearce DA, Mortishire-Smith RJ and Griffin JL (2011) A metabolomic comparison of mouse models of the Neuronal Ceroid Lipofuscinoses. J Biomol NMR, 49, 175–184. [PubMed: 21461951]

Scemes E and Giaume C (2006) Astrocyte calcium waves: what they are and what they do. Glia, 54, 716–725. [PubMed: 17006900]

Schultz ML, Tecedor L, Chang M and Davidson BL (2011) Clarifying lysosomal storage diseases. Trends in neurosciences, 34, 401–410. [PubMed: 21723623]

Seifert G, Schilling K and Steinhauser C (2006) Astrocyte dysfunction in neurological disorders: a molecular perspective. Nature reviews. Neuroscience, 7, 194–206. [PubMed: 16495941]

Sitter B, Autti T, Tyynela J et al. (2004) High-resolution magic angle spinning and 1H magnetic resonance spectroscopy reveal significantly altered neuronal metabolite profiles in CLN1 but not in CLN3. Journal of neuroscience research, 77, 762–769. [PubMed: 15352223]

Sofroniew MV and Vinters HV (2010) Astrocytes: biology and pathology. Acta neuropathologica, 119, 7–35. [PubMed: 20012068]

Stephen TL, Gupta-Agarwal S and Kittler JT (2014) Mitochondrial dynamics in astrocytes. Biochemical Society transactions, 42, 1302–1310. [PubMed: 25233407]

Stobart JL and Anderson CM (2013) Multifunctional role of astrocytes as gatekeepers of neuronal energy supply. Frontiers in cellular neuroscience, 7, 38. [PubMed: 23596393]

Takaki J, Fujimori K, Miura M, Suzuki T, Sekino Y and Sato K (2012) L-glutamate released from activated microglia downregulates astrocytic L-glutamate transporter expression in neuroinflammation: the 'collusion' hypothesis for increased extracellular L-glutamate concentration in neuroinflammation. Journal of neuroinflammation, 9, 275. [PubMed: 23259598]

Tan B, Xiao H, Li F, Zeng L and Yin Y (2015) The profiles of mitochondrial respiration and glycolysis using extracellular flux analysis in porcine enterocyte IPEC-J2. Anim Nutr, 1, 239–243. [PubMed: 29767164]

Thiele DL, Kurosaka M and Lipsky PE (1983) Phenotype of the accessory cell necessary for mitogen-stimulated T and B cell responses in human peripheral blood: delineation by its sensitivity to the lysosomotropic agent, L-leucine methyl ester. Journal of immunology, 131, 2282–2290.

Ullian EM, Sapperstein SK, Christopherson KS and Barres BA (2001) Control of synapse number by glia. Science, 291, 657–661. [PubMed: 11158678]

van der Hel WS, Notenboom RG, Bos IW, van Rijen PC, van Veelen CW and de Graan PN (2005) Reduced glutamine synthetase in hippocampal areas with neuron loss in temporal lobe epilepsy. Neurology, 64, 326–333. [PubMed: 15668432]

Vercellino M, Merola A, Piacentino C, Votta B, Capello E, Mancardi GL, Mutani R, Giordana MT and Cavalla P (2007) Altered glutamate reuptake in relapsing-remitting and secondary progressive multiple sclerosis cortex: correlation with microglia infiltration, demyelination, and neuronal and synaptic damage. Journal of neuropathology and experimental neurology, 66, 732–739. [PubMed: 17882017]

Vesce S, Rossi D, Brambilla L and Volterra A (2007) Glutamate release from astrocytes in physiological conditions and in neurodegenerative disorders characterized by neuroinflammation. Int Rev Neurobiol, 82, 57–71. [PubMed: 17678955]

Volterra A, Liaudet N and Savtchouk I (2014) Astrocyte Ca(2)(+) signalling: an unexpected complexity. Nature reviews. Neuroscience, 15, 327–335. [PubMed: 24739787]

Wang F, Smith NA, Xu Q, Fujita T, Baba A, Matsuda T, Takano T, Bekar L and Nedergaard M (2012) Astrocytes modulate neural network activity by Ca(2)+-dependent uptake of extracellular K+. Sci Signal, 5, ra26. [PubMed: 22472648]

Williams RE, Aberg L, Autti T, Goebel HH, Kohlschutter A and Lonnqvist T (2006) Diagnosis of the neuronal ceroid lipofuscinoses: an update. Biochimica et biophysica acta, 1762, 865–872. [PubMed: 16930952]

Williams RE and Mole SE (2012) New nomenclature and classification scheme for the neuronal ceroid lipofuscinoses. Neurology, 79, 183–191. [PubMed: 22778232]

Xiong J and Kielian T (2013) Microglia in juvenile neuronal ceroid lipofuscinosis are primed toward a pro-inflammatory phenotype. Journal of neurochemistry, 127, 245–258. [PubMed: 23919525]

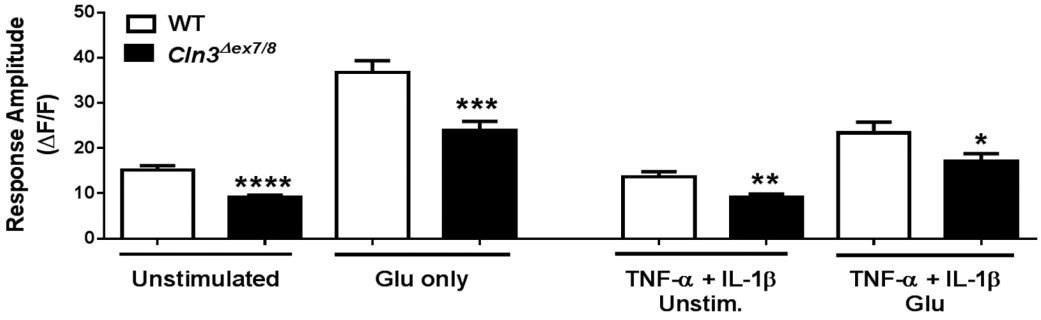

Figure 1. *CLN3* mutation alters astrocyte Ca^{2+} responses.

Primary WT and *Cln3*$^{\Delta ex7/8}$ astrocytes were unstimulated or treated with TNF-α and IL-1β (10ng/mL each) for 24 h and loaded with the Ca^{2+} indicator dye Fluo4-AM. Following a 5 min period for baseline readings, cells were exposed to 10mM glutamate (Glu) and the amplitude of the first Ca^{2+} response was calculated. Results are presented as the mean ± standard error of the mean (SEM) combined from three independent experiments with a total of 9 biological replicates (*, $p < 0.05$; **, $p < 0.01$; ****, $p < 0.0001$; Student's *t*-test).

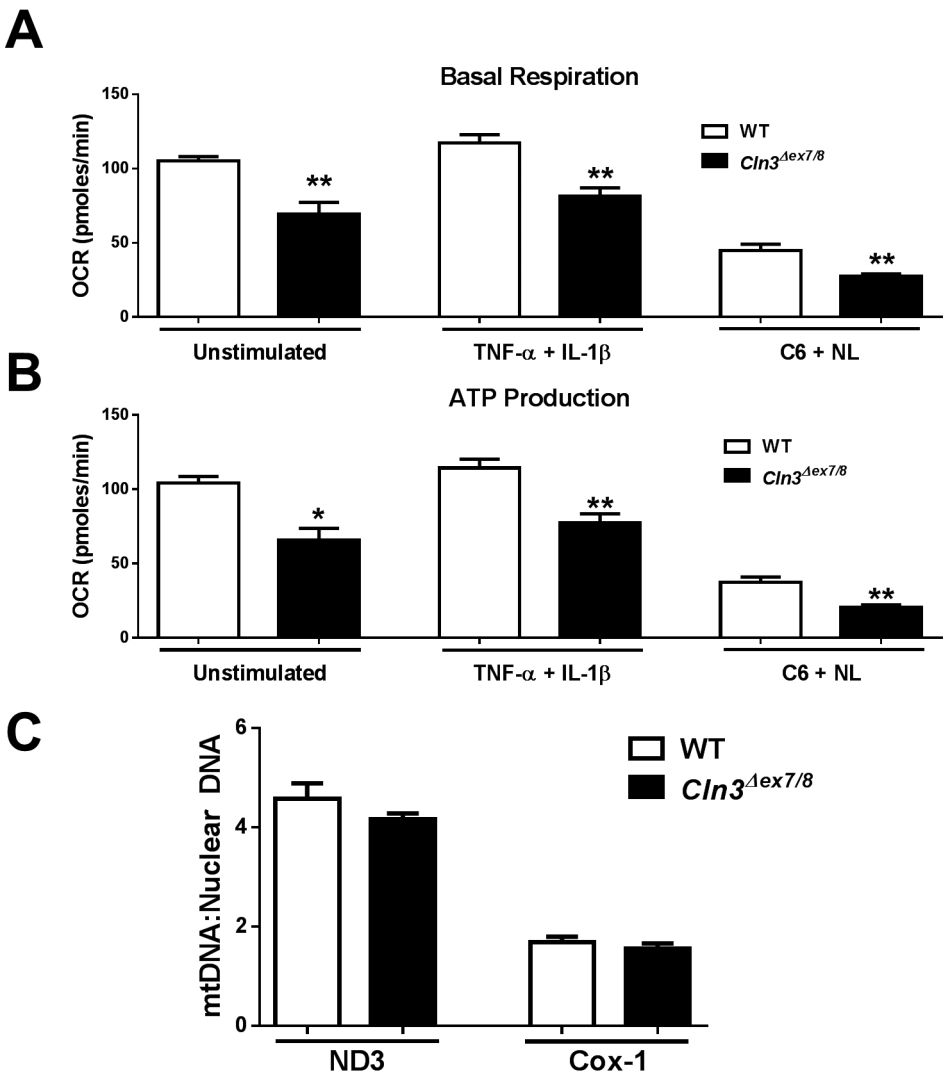

Figure 2. Mitochondrial respiration is impaired in *Cln3*$^{\Delta ex7/8}$ astrocytes.

Primary WT and *Cln3*$^{\Delta ex7/8}$ astrocytes were unstimulated or treated with TNF-α and IL-1β (10ng/mL each) or C6 ceramide (5μM) and neuronal lysate (NL) for 24 h, whereupon oxidative phosphorylation (Ox Phos) activity was examined using Seahorse Bioscience assays. (A) Basal mitochondrial respiration and (B) ATP production was determined based on oxygen consumption rate (OCR). Results are representative of three independent experiments with a total of 3 biological replicates (mean ± standard error of the mean (SEM). (C) Mitochondrial biomass was determined by quantiating NADH dehydrogenase 3 (ND3) and cytochrome c oxidase subunit-1 (Cox-1) expressed as a ratio to genomic DNA. Results are presented as the mean ± SEM of 4 biological replicates. Significant differences between WT and *Cln3*$^{\Delta ex7/8}$ astrocytes are denoted by asterisks (*, $p < 0.05$; **, $p < 0.01$; Student's *t*-test).

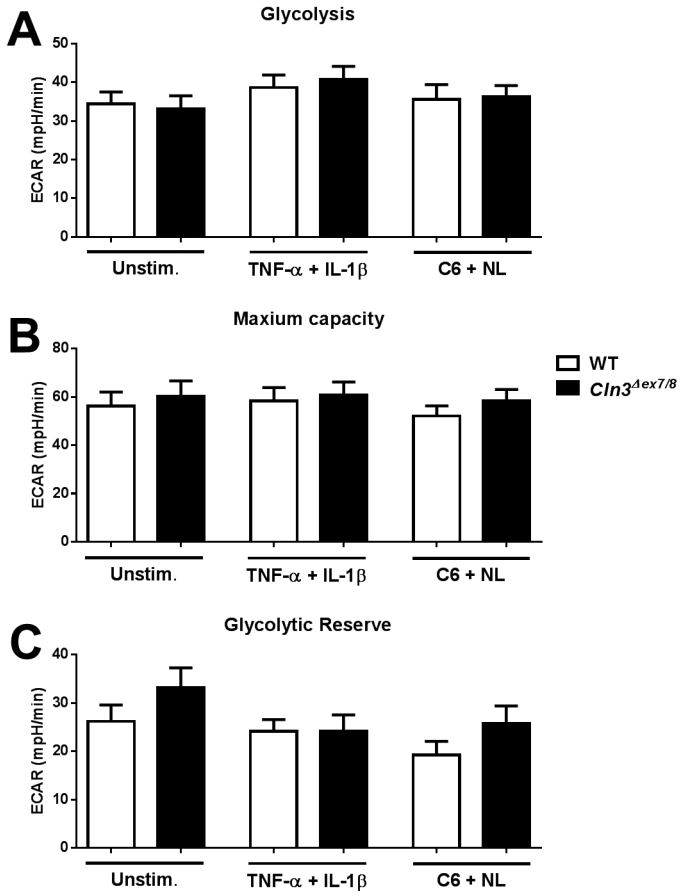

Figure 3. *CLN3* mutation does not affect astrocyte glycolytic activity.

Primary WT and *Cln3*$^{\Delta ex7/8}$ astrocytes were unstimulated or treated with TNF-α and IL-1β (10ng/mL each) or C6 ceramide (5μM) and neuronal lysate (NL) for 24 h, whereupon glycolytic activity was examined using Seahorse Bioscience assays. (A) Glycolysis, (B) Maximum capacity, and (C) Glycolytic reserve was determined based on extracellular acidification rate (ECAR). Results are representative of three independent experiments with a total of 3 biological replicates (mean ± standard error of the mean (SEM).

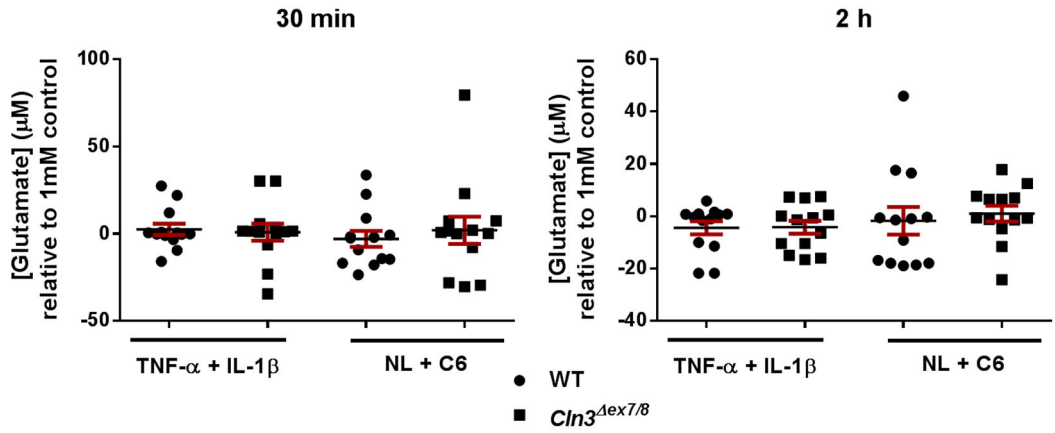

Figure 4. Glutamate uptake is not altered in *Cln3*$^{\Delta ex7/8}$ astrocytes.

Primary WT and *Cln3*$^{\Delta ex7/8}$ astrocytes were treated with TNF-α and IL-1β (10ng/mL each) or C6 ceramide (5μM) and neuronal lysate (NL) for 24 h. Cells were then exposed to 1mM glutamate, whereupon supernatants were collected 30 min and 2 h later to evaluate residual extracellular glutamate concentrations. Results were normalized to the 1mM glutamate control and are presented as the mean ± standard error of the mean (SEM) combined from three independent experiments with a total of 3 biological replicates.

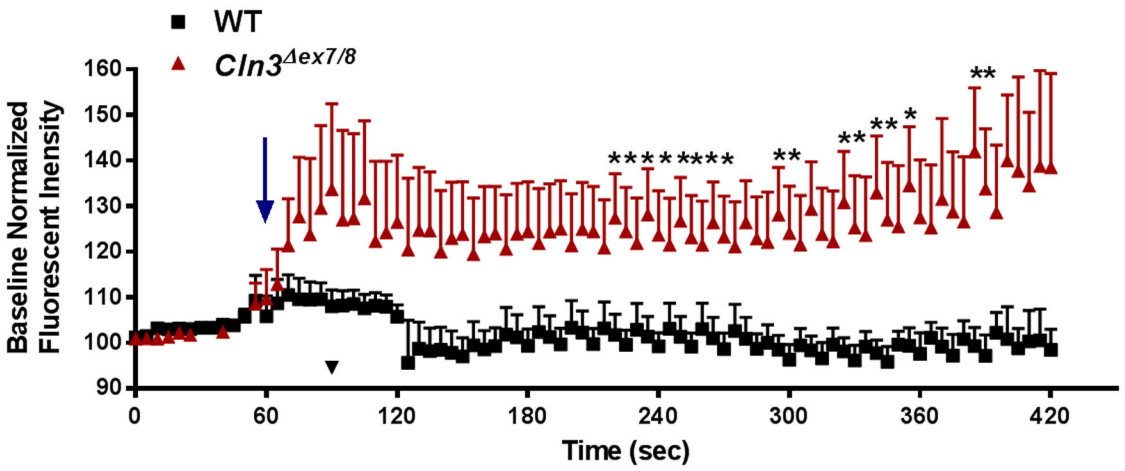

Figure 5. Ca^{2+} signaling is disrupted in *Cln3*$^{\Delta ex7/8}$ neurons.

Primary WT and *Cln3*$^{\Delta ex7/8}$ neurons were loaded with the Ca^{2+} indicator dye Fluo4-AM. Following a 5 min period for baseline recordings, neurons were treated with 25nM L-glutamic acid and evaluated for a 420 sec period. Measurements were obtained using AxioVision software with fluorescent intensity normalized to baseline values. Results are presented as the mean ± standard error of the mean (SEM) combined from three independent experiments with a total of 3 biological replicates (*, $p < 0.05$; Student's *t*-test). The arrow depicts the point of L-glutamic acid addition.

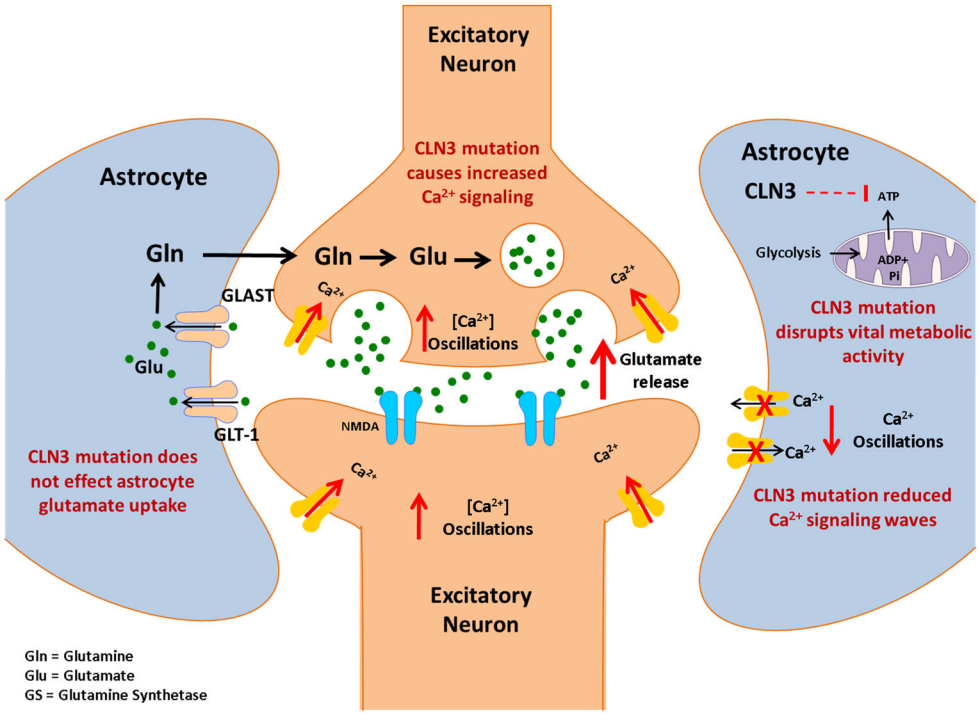

Figure 6. Proposed mechanism for aberrant astrocyte-neuron crosstalk during CLN3 disease.

Glutamate uptake by astrocytes is an energy-demanding process and ATP production was significantly decreased in *Cln3*$^{\Delta ex7/8}$ astrocytes, which coincided with impaired Ca^{2+} signaling. *Cln3*$^{\Delta ex7/8}$ neurons were hyper-sensitive to physiological concentrations of glutamate, which elicited heightened and prolonged Ca^{2+} signals that with time may contribute to neuronal dysfunction and/or death. Gln, glutamine; Glu, glutamate; GLAST, glutamate-aspartate transporter; GLT-1, glutamate transporter 1.